Volume collapse in $LaMnO_3$ studied using an anisotropic Potts model

Mahrous R. Ahmed[1,2,*] and G. A. Gehring[2]
[1]*Department of Physics, Faculty of Science, Sohag University, Sohag 82534, Egypt*
[2]*Department of Physics and Astronomy, University of Sheffield, Hicks Building, Hounsfield Road, Sheffield S3 7RH, United Kingdom*
(Received 25 September 2008; revised manuscript received 15 April 2009; published 7 May 2009)

We have investigated the volume collapse occurring in $LaMnO_3$ unit cell using the anisotropic Potts model modified by two types of anisotropic interactions which has been used to study the behavior of the orbital-ordering configurations with temperature. The bond lengths are related to the occupation of the orbits. We have shown that the collapse is due to the change of Mn-O bonds as the temperature is raised through the transition. These results are in good agreement with the recently published experimental results.

DOI: 10.1103/PhysRevB.79.174106 PACS number(s): 05.10.Ln, 75.30.Kz, 05.70.Fh, 64.60.Cn

I. INTRODUCTION

Transition-metal oxides comprise many fascinating properties and theoretical challenges that are connected with the orbital degree of freedom which is present in ions like Mn^{3+} and V^{3+}, for example, where the outer d electrons can choose between different orbitals or linear combination of these. As a consequence of strong local interactions (strong correlations) the compounds $LaMnO_3$ and $LaVO_3$ are Mott insulators and the orbital occupation and also its fluctuations strongly influence the magnetic and other properties of these systems.

$LaMnO_3$, in which Mn ions are Mn^{3+}, has an antiferromagnetic insulating ground state. Mn^{3+} ions in each MnO_6 octahedra are in its $t_{2g}^3 e_g^1$ state. A cooperative Jahn-Teller (JT) distortion removes the degeneracy of the e_g orbital and stabilizes $d_{3x^3-r^2}/d_{3y^3-r^2}$ orbitals which are ordered. The local JT distortions around each Mn^{3+} ion interact with each other cooperatively and give rise to the observed long-range orbital ordering, see Fig. 1(a).

A complete understanding of the mechanism stabilizing the observed order in the insulating mother compound $LaMnO_3$ is a prerequisite to fully understand the complex interplay among the spin, charge, orbital, and lattice degrees of freedom in the doped manganites. Hole-doped $LaMnO_3$, $La_{1-x}A_xMnO_3$ (A=Ca, Sr, and Ba), exhibits colossal magnetoresistance and has attracted very much interest through the last 50 years.[1,2] For this reason a large number of theoretical investigations has already been undertaken on stoichiometric $LaMnO_3$ itself.[3] $LaMnO_3$ crystallizes in the orthorhombic space group *Pbnm* and undergoes a transition at $T_{JT} \approx 750$ K from the Jahn-Teller-distorted orthorhombic phase to a high-temperature orthorhombic phase which is nearly cubic.[4] The low-temperature phase has three Mn-O bond lengths called short (s), medium (m), and long (l).[5] The space group *Pbnm* remains the same in both phases, but the distortion is nearly removed in the high-temperature phase. The transition is accompanied by an orbital order-disorder transition.

During their recent investigation Chatterji *et al.*[6] discovered an unusual abrupt volume contraction at $T_{JT} \approx 750$ K. The high-temperature phase just above T_{JT} has less volume than the low-temperature phase. This volume contraction is very rare in solid-solid structural phase transition. A well-known example is the volume contraction in Fe (Ref. 7) at the bcc-to-fcc (α-Fe to γ-Fe) structural transition at $T_c \approx 1185$ K. However, this volume contraction in Fe is due to the transition from the relatively open bcc structure to the closed-packed fcc structure. The volume contraction is known at the melting transition in hydrogen-bonded hexagonal ice[8] and the covalent tetrahedrally bonded Si and Ge,[9] and also in Bi, Ga, Ce, and Pu.[9]

Chatterji *et al.*[6] investigated the Jahn-Teller transition in $LaMnO_3$ using high-temperature x ray and neutron diffraction on powder samples. They observed that the unit-cell volume of $LaMnO_3$ decreases with increasing temperature in a narrow temperature range below T_{JT} and then undergoes a sudden collapse at T_{JT}. It was argued that this striking volume collapse is caused by the orbital order-disorder transition. In the orbitally ordered phase the packing of MnO_6 octahedra needs more space than in the disordered phase.

In another paper, Chatterji *et al.*[10] obtained volume contraction in Ca-doped $LaMnO_3$ doped for x=0.025 and 0.075

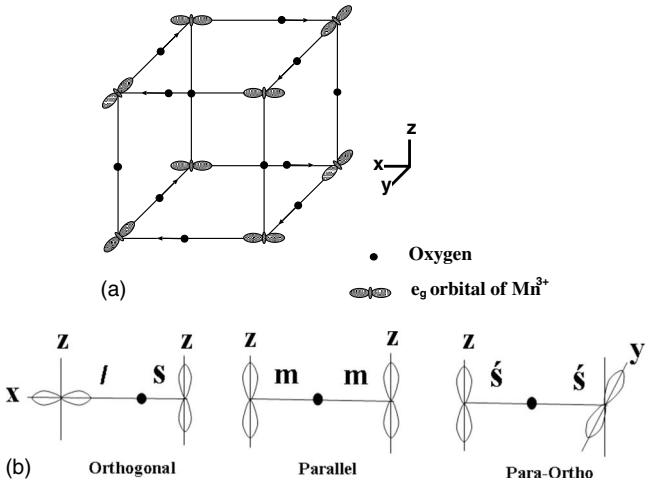

FIG. 1. (a) The orbital ordering in $LaMnO_3$. It is antiferromagnetic in the x-y plane and ferromagnetic along the $\hat{z}$ direction, (b) the three different Mn-O bonds l, m, and s (Ref. 5). The orthogonal configuration has a long and short bond, the side-side (parallel) configuration has two medium bonds. The bond lengths for the parallel-orthogonal configuration, s', have not been measured directly because this configuration does not occur in the ground state. The solid circles represent oxygen.

with temperature investigated by the same previous way. Bozin *et al.*[11] also obtained the volume contraction for the same compound as function of doping range $x=0.0$ to 0.5 at fixed $T=550$ K and as function of temperature at fixed doping $x=0.0$. They investigated their compound by advent of high data throughput neutron powder diffractometers.

Sánchez *et al.*[12] showed by means of x-ray absorption near-edge structure and extended x-ray absorption fine structure at the Mn K edge that the structural transition originates by the ordering of tetragonally distorted octahedra and they obtained the change of entropy for the orbital-ordering transition at T_{JT} comparable with the entropy of the three-state Potts model at high temperature[13–15] with nearest-neighbor antiferrodistortive coupling. It is confirmed[16] by using neutron-diffraction data and a combined Rietveld and high real-space resolution atomic-pair distribution function analysis that the nature of the JT transition around T_{JT} is to be orbital order-disorder and the intermediate structure suggests the presence of local-ordered clusters implying strong nearest-neighbor JT antidistortive coupling.

Theoretically, Maitra *et al.*[17] constructed a model Hamiltonian involving the pseudospin of Mn^{3+} e_g states, the staggered JT distortion and the volume strain coordinate to study the volume collapse of $LaMnO_3$ at the JT transition temperature. They also have shown that the anharmonic coupling between these primary- and secondary-order parameters leads to the first-order JT phase transition associated with a comparatively large reduction of the unit-cell volume.

Millis[18] derived a classical model, which was based on previous work by Kanamori,[5] for the lattice distortions in manganites. The model may be approximated either by an antiferromagnetic xy model with a modest threefold anisotropy or by a three-state Potts model with an antiferromagnetic first-neighbor interaction and a weak second-neighbor interaction. This differs from our model which deals only with the nearest-neighbor interaction.

Because we have obtained good values for the entropy[19] above T_{JT} which agree very well with the experimental results,[12] we investigate further the physical quantities arising due to the orbital order-disorder in $LaMnO_3$. We use the theory of the anisotropic Potts model developed in our previous papers[19,20] to investigate the temperature dependence of the lattice volume occurring in $LaMnO_3$. The model proposed for the disordered phase is an array of localized distortions with no long-range order. It is well known that the phenomenological models such as pseudospin or Potts models are very useful to study order-disorder transitions. The standard three-state Potts model alone does not have the correct orbital ordering for $LaMnO_3$ as a possible ground state but this arises naturally in the anisotropic model. Our earlier paper[19] showed that this phenomenological model gave the correct ground state for the orbital ordering, and in this paper we show that we also obtain good results for the volume change in the $LaMnO_3$ phase.

We explain the model in brief in Sec. II A and the Monte Carlo (MC) simulation condition in Sec. II B. The results are discussed in Sec. III and finally are concluded in Sec. IV.

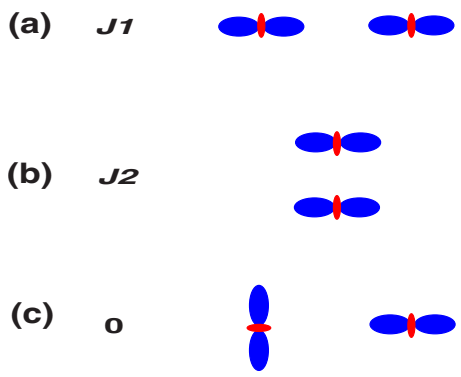

FIG. 2. (Color online) The types of the orbital interaction energy used in our simulation. (a) J_1 is the head-to-head configuration, (b) J_2 is the energy of two orbits in parallel, and (c) the interaction energy of two different orbits is chosen to be zero.

II. METHODOLOGY

A. Model

A three-state Potts model in three dimensions allows for the possibility that the Potts states and the space coordinates are coupled. This arises physically where there is strong Jahn-Teller coupling of an electronic doublet typically from d electrons coupled to the two-dimensional lattice distortions with strong unharmonic terms as discussed by Kanamori.[5] This leads to three orbits which are used as the three states of the Potts model,

$$|x\rangle = (3x^2 - r^2)f(r),$$

$$|y\rangle = (3y^2 - r^2)f(r),$$

$$|z\rangle = (3z^2 - r^2)f(r), \tag{1}$$

where $f(r)$ is a radial function and $r^2=x^2+y^2+z^2$.

In such a model the interaction between orbits depends on both the type of orbit and the direction of the bond between them.[21] The compound $LaMnO_3$ has orbital order of this type, as seen in Fig. 1(a), and the interactions between the orbits have been calculated.[22–24]

We define the anisotropic three-dimensional Potts model in terms of two interactions, J_1 and J_2 indicated in Fig. 2. The interaction J_1 is for two sites occupied by the same orbit (a head-to-head configuration), and the interaction J_2 is when the orbits are separated by a bond in one of the other directions (a side-to-side configuration).

The anisotropic three-state Potts model Eq. (2) on a simple cubic lattice is given as

$$H_{AIS} = -\frac{1}{2}\sum_{\langle i,j\rangle} J_{ii}(\underline{\rho}_{ij})\delta_{ij}, \tag{2}$$

where $\underline{\rho}_{ij}=\underline{R}_i-\underline{R}_j$ is the bond distance between i and j sites. The factor of 1/2 is included to correct for double counting.

These orbits, shown in Eq. (1), are found from the e_g doublet for the case $\theta=0\pm\frac{2\pi}{3}$.

$$|\theta\rangle = \cos\frac{\theta}{2}|3z^2 - r^2\rangle + \sin\frac{\theta}{2}|x^2 - y^2\rangle. \quad (3)$$

Experimentally[25] it is found that if the tetragonal axis is along $\hat{z}$ direction, then, the staggered orbits are given by $|\pm\theta_{\rm exp}\rangle$, where $\theta_{\rm exp}$ is closer to $\pi/2$ than $2\pi/3$. We note that

$$\left|\pm\frac{\pi}{2}\right\rangle = \cos\frac{\pi}{4}|3z^2 - r^2\rangle + \sin\frac{\pi}{4}|x^2 - y^2\rangle. \quad (4)$$

This gives, when $|-\frac{\pi}{2}\rangle$ is used, $\frac{1}{\sqrt{6}}|2.7x^2-0.7y^2-2z^2\rangle$ which has its main lobe along $\hat{x}$ direction. Similarly, using $|+\frac{\pi}{2}\rangle$ gives a state, $\frac{1}{\sqrt{6}}|2.7y^2-0.7x^2-2z^2\rangle$, which has its main lobe along $\hat{y}$ direction. We use the states given in Eq. (1), our phenomenological model because these allow us to use the same states below $T_{\rm JT}$ for any of the three possible **Q** vectors, (110), (101), and (011), and also above $T_{\rm JT}$. If we start our simulation from $T=0$ we can choose a specific configuration for the orbital-ordering ground state. If we start our simulation from high temperature we obtain any of the three possible configurations for the orbital-ordering ground state. The symmetry is broken at T_C so that the Monte Carlo simulations give one of the possible ground states and not an average of all of them.

B. Monte Carlo simulation

This model has been studied using MC simulations on $3d$ finite lattices with periodic boundary conditions (with size L^3 where $L=12$) where J_1 is negative and J_2 is small and positive. Earlier[19] we found that the values of J_1 and J_2 as $1.4 > |J_1| > 0.3$ eV and $J_2 \approx 0.12$ eV fitted the thermodynamic properties. The theory depends only on the ratio J_2/J_1. Our phase occurs within the range $0 < |J_2/J_1| < 0.5$, where $J_1 = -1$ (see phase 5 of our earlier work[20]). In this simulation we chose $|J_2/J_1| = 0.02$ where the transition is stronger first order. All our simulations have made use of the Metropolis algorithm with averaging performed over from 10^5 to 10^7 Monte Carlo steps per site. Results were obtained by either cooling down from a high-temperature random configuration as discussed by Banavar *et al.*[26] or heating up from the ground state. The results from the two procedures agree.

III. RESULTS AND DISCUSSION

In our previous work we have used the modified Potts model to obtain the orbital ordering in $LaMnO_3$ and now in this paper we study the volume collapse occurring due to the orbital-order disordering in $LaMnO_3$. The occupation of the orbitals given in Eq. (1) on Mn neighboring sites affects the Mn-Mn separation as shown in Fig. 2.

We obtained the occupations of the orbits from the Monte Carlo simulation and hence the three probabilities for the orbital configurations shown in Fig. 2.

The orbital ordering in the ground state of $LaMnO_3$ is shown in Fig. 1(a). We now use the bond lengths to relate these to the volume. The experimental[4] values of l, m, and s are the following: $l=2.178$ Å, $m=1.968$ Å, and $s=1.907$ Å. The two bonds which are between the two orbitals of the orthogonal configuration are long and short, $l+s$, between the two orbitals of the side-side configuration are two mediums, $2m$, and finally between the orbitals of the parallel-orthogonal configuration are two shorts, $2s$. The separation between parallel orthogonal has not been measured experimentally. For separation $2s'$ between parallel-orthogonal bonds we assumed that $s=s'$.[5] We note that the lengths of the short and medium bonds are quite similar whereas the long bond is significantly longer. The lobe of the Mn d orbital is pointing away from the oxygen in the short bond of the orthogonal, the side-side and parallel-orthogonal configurations.[5] The bond lengths, short and medium, differ slightly. We assume that this is because of the Coulomb repulsion between the d orbitals in the side-side configuration and so choose the bond length for the parallel orthogonal, s', to equal that of the short bond, s. The volume of the $LaMnO_3$ unit cell in the ground state is given by

$$\text{volume} = (l+s)(l+s)(m+m) = (l+s)^2(2m). \quad (5)$$

To calculate the $LaMnO_3$ lattice volume we do the following. We calculate the probabilities to obtain each configuration along each axis, then, multiply these probabilities in the real bond lengths between the two orbitals of each configuration. Along x axis we get the average of lattice edge length:

$$\langle a_x(T)\rangle = P_{o_x}(l+s) + P_{(s\text{-}s)_x}(2m) + P_{(p\text{-}o)_x}(2s) \quad (6)$$

and equivalently for the y and z axes. The volume of $LaMnO_3$ unit cell is,

$$\text{volume}(T) = \langle a_x(T)\rangle\langle a_y(T)\rangle\langle a_z(T)\rangle. \quad (7)$$

These simulations start from the state shown in Fig. 1(a) at low temperature, and the temperature is increased. The probability for each configuration along x and y axes are equal and above $T_{\rm JT}$ the three axes become equivalent at all temperatures. Figure 3 shows the probabilities of the (a) orthogonal, (b) side-side, and (c) parallel-orthogonal configurations along x, y, and z axes. There is a unit probability for an orthogonal bond along x and y axes at $T=0$ and this probability falls with increasing temperature as shown in Fig. 3(a) which also shows that the probability for an orthogonal bond along the z axis rises as the temperature increases. Figure 3(b) shows the equivalent result for the side-side configuration which is the only one present along the z axis at $T=0$. The parallel-orthogonal configuration is zero for all axes at low temperature and increases with temperature with different increase rate for the z axis from the x and y axes but these probabilities remain small as shown in Fig. 3(c).

The average of the configurations probability is given by double of probability along x axis plus probability along z axis. There are almost no head-head bonds in any direction at the temperature range studied here, this is what gives rise to the reduced entropy at $T_{\rm JT}$.

Figure 3(d) shows that the sum of decreasing rate of the orthogonal configuration in x and y axes is equal to the increasing rate of the orthogonal configuration in z axis so that the total probability of the orthogonal configuration is almost independent of temperatures. The decrease in the rate of the probability of side-side configuration is bigger in z axis than the increasing rate of the probability of the side-side in x and y axes so that the total probability of side-side configuration

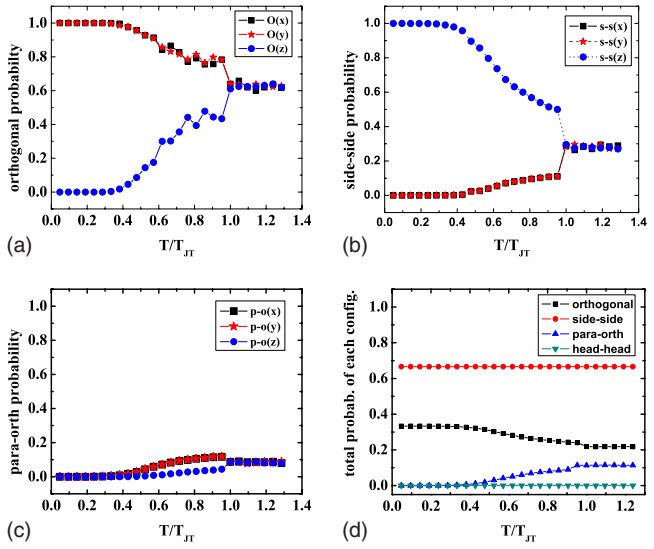

FIG. 3. (Color online) (a) The probability of orthogonal configuration along the three axes, (b) the probability of side-side configuration along the three axes, (c) the probability of parallel-orthogonal configuration along the three axes, and (d) the total probability of each configuration as function of temperature. Note that net side-side ($2m$) decreases and net para-orth ($2s$) increases. Hence, volume change depends on $(m-s)$ which is small. The plots are for $J_1=-1$ and $J_2=0.02$.

decreases slowly with temperature as shown in Fig. 3(d). Finally, because the probability of parallel orthogonal is increasing in the three axes, the total probability is also increasing.

The volume change, ΔV_{theor}, which is obtained after we subtract $V(T)$ from $V(T_{\text{JT}})$ of the unit cell of $LaMnO_3$, obtained from Eq. (7) and which is plotted as a function of the reduced temperature, T/T_{JT}, is shown in Fig. 4(a). It does change slightly in the ordered phase, then it collapses dramatically at T_{JT} at the first-order transition. This result for the volume collapse in $LaMnO_3$ at T_{JT} is in an agreement, within the errors, with the experimental results[6] shown in Fig. 4(b). Our ΔV_{theor} is 1/4 of the volume of that defined in Chatterji,[6] with very small error, where they included the lattice distortions in their results and used a unit cell four times bigger than our unit cell.

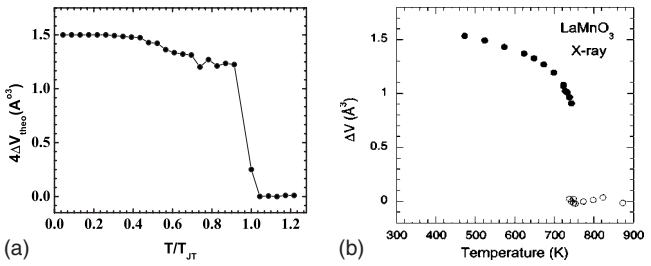

FIG. 4. (a) Calculated temperature dependence of ΔV_{theor} of $LaMnO_3$ unit cell, where $\Delta V_{\text{theor}}=V(T)-V(T_{\text{JT}})$. The errors size is smaller than the symbol size. The line is a guide to the eye. The plot is for $J_1=-1$ and $J_2=0.02$ (b) measured temperature variation of the unit-cell volume after subtraction of the base volume (this figure is taken from Ref. 6).

IV. CONCLUSION

The Potts model with two anisotropic orbital interaction types, J_1 and J_2 has produced the orbital-ordering phase which occurs in $LaMnO_3$ at specific values of J_1 and J_2. It was obtained also from the same model the internal energy and specific heat for the same phase.[20] The model also has produced good results for the order parameter and values for the entropy at orbital-ordering phase-transition temperature T_{JT} confirmed by experiment.

In this paper, using the same model refined to include the relation of the orbits to the bond lengths, we calculated the volume change with the temperature that occurs at T_{JT} in $LaMnO_3$ which has been studied by Chatterji *et al.*[6] It was found that the volume of the $LaMnO_3$ unit cell collapses dramatically at T_{JT} at the first-order transition. This model showed that this is due to the decrease in number of the medium Mn-O bonds and the corresponding increase in the number of the short Mn-O bonds as the lattice is warmed through T_{JT}. The theoretical volume which is calculated here was found equal to 1/4 of the experimental volume where the lattice distortion was considered in the experimental results and a unit cell four times bigger than our unit cell was used.

The model needs more modifications to be able to calculate the behavior of $LaMnO_3$ lattice distortion parameters and in their results and used a unit cell four times bigger than our unit cell Mn-O bond lengths with the temperature.

ACKNOWLEDGMENTS

This work was funded by both the University of Sohag, Egypt, and the University of Sheffield, UK.

*Corresponding author. mahrous_r_ahmed@yahoo.com

[1] Y. Tokura and N. Nagaosa, Science **288**, 462 (2000).

[2] *Colossal Magnetoresistive Oxides*, edited by Y. Tokura (Gordon and Breach, New York, 2000).

[3] A. J. Millis, Phys. Rev. B **53**, 8434 (1996); S. Ishihara, J. Inoue, and S. Maekawa, *ibid.* **55**, 8280 (1997); S. Okamoto, S. Ishihara, and S. Maekawa, *ibid.* **65**, 144403 (2002); L. F. Feiner and A. M. Olés, *ibid.* **59**, 3295 (1999); J. Bala and A. M. Olés, *ibid.* **62**, R6085 (2000); J. E. Medvedeva, M. A. Korotin, V. I. Anisimov, and A. J. Freeman, *ibid.* **65**, 172413 (2002).

[4] J. Rodriguez-Carvajal, M. Hennion, F. Moussa, A. H. Moudden, L. Pinsard, and A. Revcolevschi, Phys. Rev. B **57**, R3189 (1998).

[5] J. Kanamori, J. Appl. Phys. **31**, S14 (1960).

[6] T. Chatterji, F. Fauth, B. Ouladdiaf, P. Mandal, and B. Ghosh, Phys. Rev. B **68**, 052406 (2003).

[7] Y. S. Touloukian *et al.*, *Thermal Expansion of Metallic Elements and Alloys* (Plenum, New York, 1977).

[8] V. F. Petrenko and R. W. Whitworth, *Physics of Ice* (Oxford University Press, Oxford, 2002).
[9] T. Iida and R. I. L. Guthrie, *Physical Properties of Liquid Metals* (Clarendon, Oxford, 1988).
[10] T. Chatterji, D. Riley, F. Fauth, P. Mandal, and B. Ghosh, Phys. Rev. B **73**, 094444 (2006).
[11] E. S. Bozin, X. Qiu, R. J. Worhatch, G. Paglia, M. Schmidt, P. G. Radaelli, J. F. Mitchell, T. Chatterji, Th. Proffen, and S. J. L. Billinge, Z. Kristallogr. **2007** (26), 429 (2007).
[12] M. C. Sánchez, G. Subías, J. García, and J. Blasco, Phys. Rev. Lett. **90**, 045503 (2003).
[13] R. B. Potts, Proc. Cambridge Philos. Soc. **48**, 106 (1952).
[14] F. Y. Wu, Rev. Mod. Phys. **54**, 235 (1982).
[15] J.-S. Wang, R. H. Swendsen, and R. Kotecky, Phys. Rev. B **42**, 2465 (1990).
[16] X. Qiu, Th. Proffen, J. F. Mitchell, and S. J. L. Billinge, Phys. Rev. Lett. **94**, 177203 (2005).
[17] T. Maitra, P. Thalmeier, and T. Chatterji, Phys. Rev. B **69**, 132417 (2004).
[18] A. J. Millis, Phys. Rev. B **53**, 8434 (1996).
[19] Mahrous R. Ahmed and G. A. Gehring, Phys. Rev. B **74**, 014420 (2006).
[20] M. R. Ahmed and G. A. Gehring, J. Phys. A **38**, 4047 (2005).
[21] J. S. Zhou and J. B. Goodenough, Phys. Rev. B **60**, R15002 (1999).
[22] T. Mizokawa, D. I. Khomskii, and G. A. Sawatzky, Phys. Rev. B **60**, 7309 (1999).
[23] D. I. Khomskii and K. I. Kugel, Phys. Rev. B **67**, 134401 (2003).
[24] J. Farrell and G. A. Gehring, New J. Phys. **6**, 168 (2004).
[25] J. Deisenhofer, B. I. Kochelaev, E. Shilova, A. M. Balbashov, A. Loidl, and H. A. Krug von Nidda, Phys. Rev. B **68**, 214427 (2003).
[26] J. R. Banavar, G. S. Grest, and D. Jasnow, Phys. Rev. B **25**, 4639 (1982).